On the Interaction of Neomycin with the Slow Vacuolar Channel of *Arabidopsis thaliana*

Joachim Scholz-Starke, Armando Carpaneto, and Franco Gambale

Istituto di Biofisica, Consiglio Nazionale delle Ricerche, 16149 Genoa, Italy

This study investigates the interaction of the aminoglycoside antibiotic neomycin with the slow vacuolar (SV) channel in vacuoles from *Arabidopsis thaliana* mesophyll cells. Patch-clamp experiments in the excised patch configuration revealed a complex pattern of neomycin effects on the channel: applied at concentrations in the submicromolar to millimolar range neomycin (a) blocked macroscopic SV currents in a voltage- and concentration-dependent manner, (b) slowed down activation and deactivation kinetics of the channel, and most interestingly, (c) at concentrations above 10 μM, neomycin shifted the SV activation threshold towards negative membrane potentials, causing a two-phasic activation at high concentrations. Single channel experiments showed that neomycin causes these macroscopic effects by combining a decrease of the single channel conductance with a concomitant increase of the channel's open probability. Our results clearly demonstrate that the SV channel can be activated at physiologically relevant tonoplast potentials in the presence of an organic effector molecule. We therefore propose the existence of a cellular equivalent regulating the activity of the SV channel in vivo.

The Journal of General Physiology

INTRODUCTION

The slow vacuolar (SV) channel is a nonselective voltage-dependent cation channel in the vacuolar membrane of all plant species investigated so far by means of the patch-clamp technique (Allen and Sanders, 1997; Demidchik et al., 2002; Scholz-Starke et al., 2005). It has been demonstrated that the slow vacuolar channel is a poorly selective cation channel permeable to both monovalent and divalent cations, namely calcium (Pantoja et al., 1992; Amodeo et al., 1994; Ward and Schroeder, 1994; Allen and Sanders, 1996; Gambale et al., 1996; Pottosin et al., 2001; Scholz-Starke et al., 2004). Moreover, the pore displays relative flexibility (Gambale et al., 1996; Scholz-Starke et al., 2004), being permeable also to organic cations (e.g. polyamines), although only under the action of large membrane potentials (Dobrovinskaya et al., 1999a,b). Therefore, a wide dimension of the narrowest pore constriction, between 5 and 8 Å, has been suggested (Gambale et al., 1996; Dobrovinskaya et al., 1999a). The SV voltage dependence exhibits a pronounced outward rectification under most experimental conditions: the channel is only active at (cytosol) positive potentials, indicating that the channel is closed at physiological tonoplast potentials, which are assumed to be slightly negative. Thus, there is a discrepancy between SV activation in patch-clamp experiments and under normal in vivo conditions. Therefore, the essential question is: which cellular parameters can shift SV activation to physiological potentials? Several possible agents have been identified in cytosolic (Hedrich and Neher, 1987; Reifarth et al., 1994; Pottosin et al., 1997) and vacuolar Ca^{2+} (Pottosin et al., 1997; Pottosin et al., 2004), cytosolic Mg^{2+} (Carpaneto et al., 2001), and the K^+ gradient across the tonoplast (Ivashikina and Hedrich, 2005). Also cytosolic pH and redox potential have been demonstrated to modulate the activation characteristics of SV channels (Schulz-Lessdorf and Hedrich, 1995; Carpaneto et al., 1999).

The SV channel was shown to be blocked by quaternary ammonium ions and Tris in a voltage-dependent manner (Dobrovinskaya et al., 1999a). Moreover, blocking efficiency of naturally occurring polyamines was dependent on their net charge, according to the sequence putrescine$^{(2+)}$ < spermidine$^{(3+)}$ < spermine$^{(4+)}$ (Dobrovinskaya et al., 1999b). Neomycin is a polyamine of the aminoglycoside antibiotics class. Its chemical structure, based on several aminated sugars joined to a dibasic cyclitol (Fig. 1), can hold up to six positive charges at acidic pH. At pH 7.4, the net charge of neomycin is +4.0 (Yeiser et al., 2004). The antibiotic effects of aminoglycosides are primarily based on their ability to bind to prokaryotic ribosomes, thereby impairing protein synthesis (Moazed and Noller, 1987; Woodcock et al., 1991). In cell biology, neomycin is widely used in studies on inositol 1,4,5-triphosphate (IP_3)–dependent intracellular calcium release, as it inhibits the IP_3-creating enzyme PLC (Downes and Michell, 1981; Gabev et al., 1989). Furthermore, neomycin was shown to block many types of animal ion

Correspondence to Joachim Scholz-Starke: scholz@ge.ibf.cnr.it

Abbreviations used in this paper: DTT, dithiothreitol; IP_3, inositol 1,4,5-triphosphate; RyR, ryanodine receptor; SV, slow vacuolar.

channels: Ca^{2+}-activated potassium channels from rat brain (Nomura et al., 1990), mechanosensitive (Winegar et al., 1996) and L-type calcium channels (Haws et al., 1996) from mouse skeletal muscle, P/Q-type calcium channels of guinea pig brain (Pichler et al., 1996), nicotinic acetylcholine receptor channels (Rothlin et al., 2000; Shi et al., 2002), the cardiac ryanodine receptor channel (Mead and Williams, 2002; Mead and Williams, 2004), rat skeletal muscle sodium channels (Yeiser et al., 2004), and neuronal vanilloid receptor channels (Raisinghani and Premkumar, 2005). Interestingly, aminoglycosides can also have activating properties, e.g., on neuronal NMDA receptors (Lu et al., 1998). From these studies it becomes evident that neomycin and other aminoglycoside antibiotics interact with a range of calcium-permeable or cationic channels that are characterized by a wide pore. This study was designed to verify if these compounds are also able to modulate the transport properties of the slowly activating vacuolar channel. The results revealed a complex pattern of both inhibitory and activating properties of neomycin on *Arabidopsis* SV channels.

MATERIALS AND METHODS

Plant Material

Plants of *Arabidopsis thaliana*, ecotype Columbia (Col-0), were grown in soil in a growth chamber at +22°C temperature and 8 h light/16 h dark regime.

Vacuole Isolation

For isolation of mesophyll protoplasts, rosette leaves of 3–5 wk old plants were used. After careful removal of the lower epidermis using fine sand paper, leaves were incubated for 30 min at 30°C in enzyme solution containing 0.8% cellulase Onozuka R-10 (Yakult), 0.08% pectolyase Y-23 (Seishin), 1 mM $CaCl_2$, 300 mM D-sorbitol, 0.5% (wt/vol) polyvinylpyrrolidone (PVP-10), 0.5% (wt/vol) BSA, 5 mM MES, pH 5.5. Protoplasts were washed two times and resuspended in bath solution. Vacuole release was observed under the microscope after adding EDTA to aliquots of protoplast solution. After settling of the vacuoles, solution was carefully replaced by fresh bath solution.

Patch-clamp Recordings and Analysis

Patch-clamp experiments were performed on isolated vacuoles in the excised cytosolic side-out patch configuration. For recordings of macroscopic currents, standard ionic solutions were as follows: 200 mM KCl, 2 mM $MgCl_2$, 2 mM $CaCl_2$, 10 mM MES/Tris, pH 5.5 in the pipette; 100 mM KCl, 2 mM $MgCl_2$, 1 mM $CaCl_2$, 1 mM dithiothreitol (DTT), 10 mM HEPES/Tris, pH 7.5 in the bath. DTT was added to the bath solution in order to prevent channel rundown (Bertl and Slayman, 1990; Carpaneto et al., 1999; Scholz-Starke et al., 2004). The osmolarity of both solutions was adjusted to 350 mOsm by the addition of D-sorbitol. In single channel experiments the bath solution contained 200 mM KCl, 2 mM $MgCl_2$, 1 mM $CaCl_2$, 1 mM DTT, 10 mM HEPES adjusted to pH 7.5 with 5.2 mM KOH; the pipette solution was identical to the one for macroscopic currents, with the exception that pH adjustment was done with 2 mM KOH instead of Tris. Appropriate concentrations of neomycin B and kanamycin A (both from Sigma-Aldrich) were reached by diluting 50 mM aqueous stock solutions that were prepared once a week, stored at 4°C, and protected from light. The bathing medium surrounding the excised patch was exchanged using a "fast perfusion system," as described previously (Carpaneto et al., 1999, 2001). Patch pipettes were pulled from thin-walled borosilicate glass (Clark Electrochemical Instruments). Ionic currents were recorded with a List EPC7 current-voltage amplifier. Data were digitized using a 16 bit Instrutech A/D/A board (Instrutech) interfaced to a MacIntosh PC, which generated the voltage stimulation protocol and archived the current response. The sign of current and voltage follows the convention proposed by Bertl et al. (1992).

Effects of neomycin were seen in all the vacuoles tested ($n = 47$). Instantaneous tail currents were evaluated from the best fit with a single exponential function. The initial current at t = 0 was denoted as I_0. I_{norm} was obtained by dividing I_0 by the maximum current derived from a Boltzmann fit of the data. In control conditions and in the presence of 0.5–50 μM neomycin, data were fitted with a single Boltzmann function ($I = I_{max}/[1 + \exp(-zF(V - V_{1/2})/RT)]$), at concentrations >200 μM by the sum of two Boltzmann functions ($I = I'_{max}/[1 + \exp(-z'F(V - V'_{1/2})/RT)] + I''_{max}/[1 + \exp(-z''F(V - V''_{1/2})/RT)]$.

Deactivation time constants were evaluated by a best fit of tail currents with a monoexponential function. Half-activation times were evaluated from the difference between the steady-state current and instantaneous current. Owing to the slower kinetics in the presence of neomycin, macroscopic currents frequently did not reach full saturation within the length of the applied voltage pulse. Consequently, the determination of steady-state levels was more difficult and activation times may be slightly underestimated.

The dose–response analysis of neomycin block was done by normalizing stationary currents recorded in the presence of neomycin by control current values ($I_{norm} = I_{neo}/I_{control}$). As I_{norm} contained a component due to the shift of the activation curve (Table I), i.e., $I_{norm} = (G_{neo}/G_{control}(block))(P_{neo}/P_{control})$, we

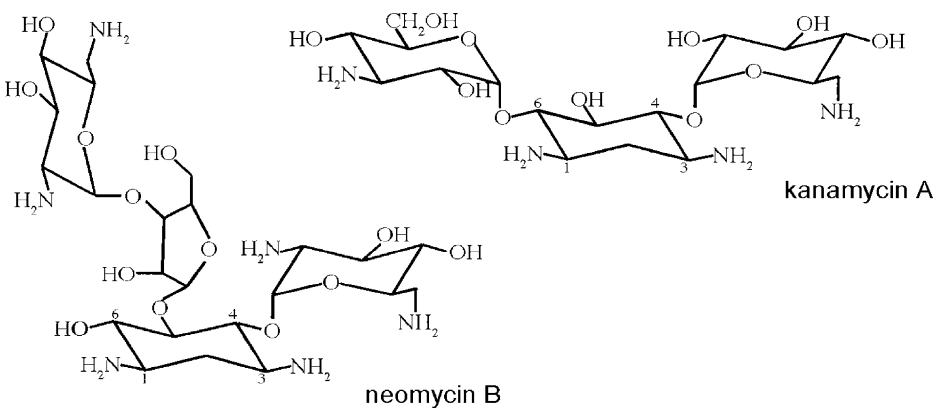

Figure 1. Structures of the aminoglycoside antibiotics used in this study. For the sake of clarity, the C atoms of the cyclitol 2-deoxystrepamine are numbered, illustrating the classification of neomycin B as a 4,5-disubstituted and of kanamycin A as a 4,6-disubstituted aminoglycoside. Modified from Mingeot-Leclercq et al. (1999).

TABLE I

Shift of the SV Activation Potential by Neomycin

[neomycin] (μM)	$V'_{1/2}$ (mV ± SEM)	z′ (±SEM)	$V''_{1/2}$ (mV ± SEM)	z″ (±SEM)	N
	First Boltzmann		Second Boltzmann		
0	+45 ± 1	2.5 ± 0.1	–	–	9
0.5	+47 ± 2	2.3 ± 0.1	–	–	3
2	+41 ± 2	2.4 ± 0.2	–	–	4
10	+35 ± 2	2.2 ± 0.2	–	–	5
50	+33 ± 3	2.0 ± 0.2	–	–	5
200	+32 ± 3	1.7 ± 0.6	−34 ± 15	4.0 ± 3.8	4
1000	+32 ± 5	1.9 ± 0.5	−44 ± 6	5.4 ± 2.6	3

Boltzmann analysis of instantaneous SV tail currents in the presence of different neomycin concentrations. Data from N experiments were averaged and subjected to a weighted best fit with one or, at neomycin concentrations >200 μM, two Boltzmann functions. Columns show the neomycin concentration, the voltage of half activation $V_{1/2}$, and the apparent gating charge z.

evaluated the real neomycin blocking efficiency by correcting the data by the following operation: $G_{neo}/G_{control}(block) = I_{norm}(P_{control}/P_{neo})$, with $(P_{control}/P_{neo}) = (1 + \exp((-z^{neo}F (V - V_{1/2}{}^{neo}))/(RT)))/(1 + \exp((-z^{control}F(V - V_{1/2}{}^{control}))/(RT)))$.

RESULTS

Neomycin Causes a Shift of the SV Activation Potential

In most experimental conditions, the SV channel activates at positive tonoplast potentials, giving rise to cationic outward currents. Likewise, currents recorded in vacuoles of *Arabidopsis thaliana* mesophyll cells showed the typical voltage-dependent characteristics of channel activation (Figs. 2 and 4). In control conditions, both macroscopic currents of a cytosolic side-out excised patch (Fig. 2 A, left) and the corresponding deactivation tail currents (Fig. 2 B, left) showed SV activation at voltages more positive than +20 mV. With 1 mM neomycin B in the bath solution, however, SV-type currents were recorded already at voltages more positive than −10 mV. Currents were first inwardly directed and correctly inverting between +10 and +20 mV (Fig. 2 A, right), as expected for a cation-selective channel from $V_{Nernst}(K^+) = +15.7$ mV. The corresponding tail current traces (Fig. 2 B, right) confirmed the presence of open SV channels already at −10 mV, absent in control conditions (Fig. 2 B, left). The results shown in Fig. 2 (A and B) suggested a shift of the SV activation potential towards negative values in the presence of neomycin. Boltzmann plots of instantaneous tail currents at −80 mV versus the prepulse voltage ranging from −80 to +100 mV are reported in Fig. 2 C. They confirmed that the presence of 1 mM neomycin enables SV activation at far more negative potentials compared to control. Investigating the Boltzmann parameters for a range of neomycin concentrations from submicromolar to millimolar values (Table I), we found that concentrations as low as 10–50 μM were sufficient to cause a shift in the half-activation potential ($V_{1/2}$) of about −10 mV, without significantly affecting the gating charge of the channel. At concentrations >200 μM, there was significant channel activation already at negative membrane potentials. In Fig. 2 C, this appears as a "shoulder" in the activation curve in the voltage range from −40 to 0 mV (see the inset with an expanded y scale). When data were fitted with a single Boltzmann function, the data points of this shoulder gave rise to the reduced steepness of the graph, without being well included into the fit. In the presence of high concentrations of neomycin, we needed to fit the data with the sum of two Boltzmann distributions (Fig. 2 C), i.e., high concentrations favor the appearance of a channel activation mechanism absent or invisible at lower antibiotic concentrations. At positive membrane potentials, the fit resulted in a gating charge value z′ that was only slightly reduced at concentrations >200 μM and a shift in $V'_{1/2}$ that was comparable to the one at 10 and 50 μM, indicating saturation already in this low concentration range (Table I). The voltage dependence of SV activation at negative potentials, on the other hand, also responded to the neomycin concentration, with $V''_{1/2}$ being shifted to more negative values at 1 mM compared to 200 μM neomycin, while the gating charge z″ did not change significantly (Table I). In summary, neomycin caused a shift of the SV activation potential to more negative values, reaching its half maximum already at low micromolar concentrations. Additionally, high concentrations of neomycin gave rise to substantial channel opening at physiological membrane potentials.

Neomycin Changes the Kinetic Properties of Macroscopic SV Currents

The presence of neomycin in the bath solution markedly changed the kinetic properties of macroscopic SV currents. Fig. 3 A shows the time required for half activation ($t_{1/2}$) at different membrane potentials. Neomycin present at 10–200 μM caused a modest increase in $t_{1/2}$, preferentially at smaller potentials. The effect on channel deactivation was much more pronounced (Fig. 3 B). While the time constant of deactivation (τ) derived from tail currents in control conditions was about 15–30 ms, its value rose dramatically with increasing neomycin concentrations, reaching hundredfold at 1 mM neomycin.

Neomycin Causes a Voltage-dependent Block of SV Currents at Positive Potentials

At membrane potentials >+20 mV, macroscopic SV-currents were strongly reduced when 1 mM neomycin was added to the bath solution (Fig. 4 A, middle, and Fig. 4 B). The degree of channel block was dependent on the applied voltage, as shown in the insets; in the presence of neomycin the current amplitude displayed a maximum at +70 mV, possibly indicating that the positively charged neomycin molecule may be driven into the pore at elevated (cytosol) positive potentials, leading to pore occlusion. Upon removal of neomycin, current

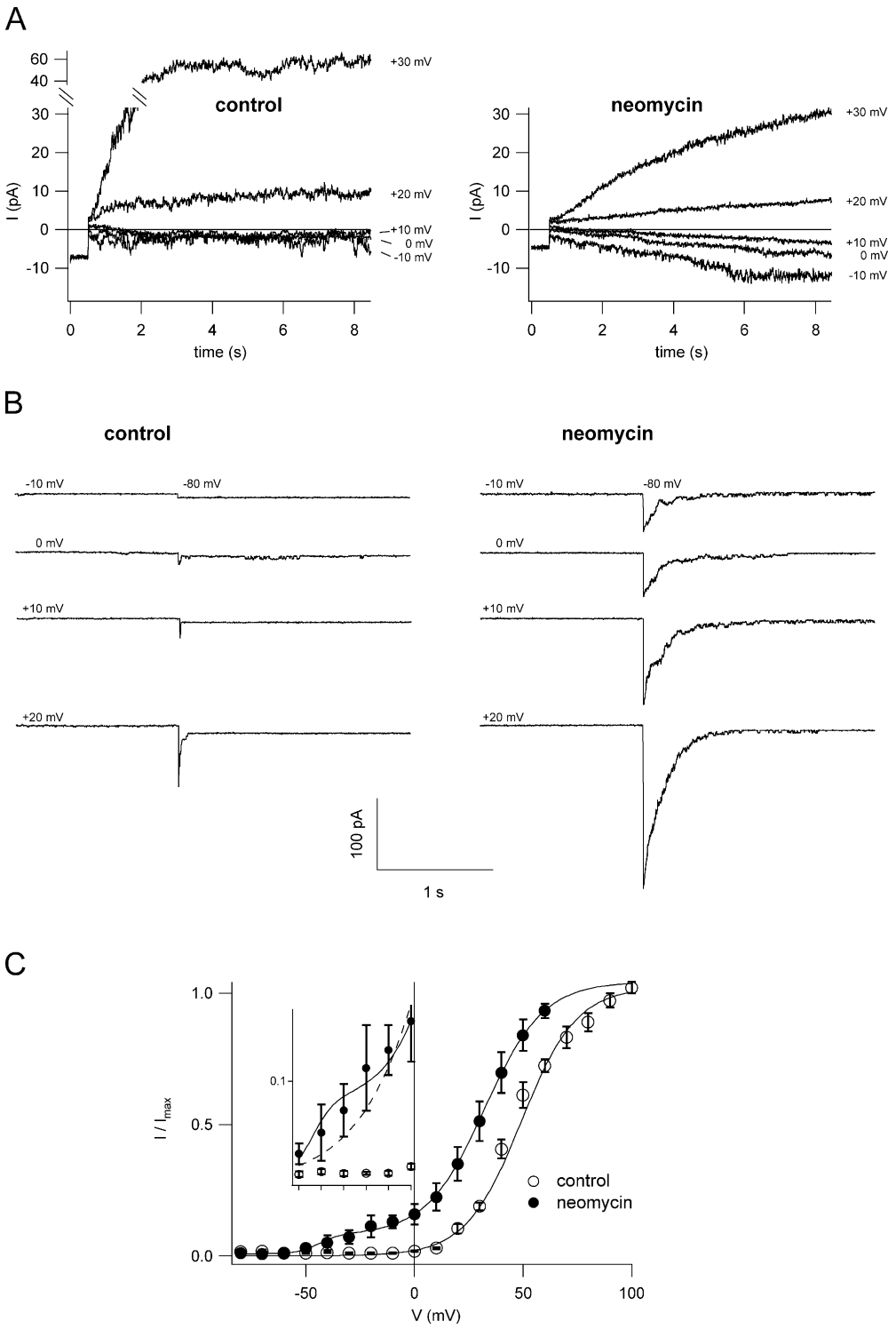

Figure 2. Neomycin shifts the voltage dependence of SV activation. (A) Traces showing SV current activation; compared to control conditions (left) neomycin (1 mM; right) activates SV channels at more negative potentials, giving rise to inward cation currents. Currents were recorded from a large cytosolic side-out vacuolar patch in bath and pipette solutions containing 100 and 200 mM K^+, respectively. (B) The threshold of SV current activation in control (left) and neomycin (1 mM, right) was probed by monitoring the deactivation tail currents upon application of the nonpermissive potential of −80 mV after a prepulse stimulus ranging from −10 to +20 mV in 10-mV steps. (C) Normalized instantaneous tail currents (see MATERIALS AND METHODS) were plotted as a function of the activating potential and fitted with a single (control; open circles) or two (1 mM neomycin; closed circles) Boltzmann functions. Data points represent the mean of seven experiments in control and three experiments in 1 mM neomycin, error bars represent SEM. Single experiment data were fitted with a Boltzmann function, normalized to the saturating current level, and averaged. In the inset, data points between –50 and 0 mV are plotted with an expanded y scale, in order to point out the "shoulder" in the normalized current data for neomycin deviating from the theoretical single Boltzmann function.

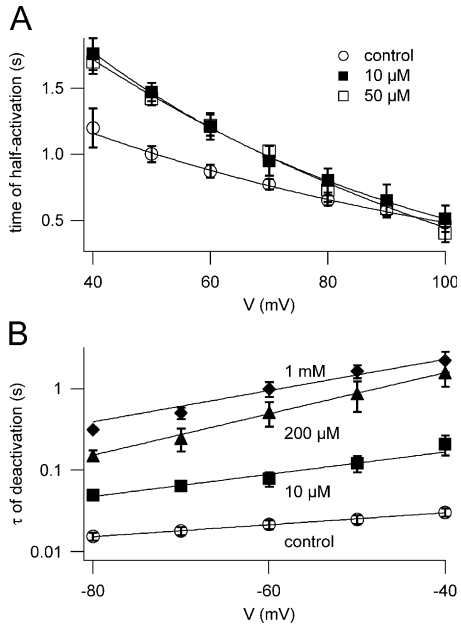

Figure 3. Neomycin slows down both activation and deactivation of macroscopic SV currents. (A) Time required for current half activation is plotted against the applied membrane potential. Data points represent mean values (± SEM) determined in control conditions (open circles; $n = 9$), in the presence of 10 μM (closed squares; $n = 5$) and 50 μM neomycin (open squares; $n = 4$). Lines are best fits to a monoexponential function. The increase of activation time saturated already at 10 μM neomycin; consequently, values for 200 μM are not given for clarity, but were comparable and overimpose to 10 and 50 μM. (B) Time constants of current deactivation τ are plotted against the tail potential. Data points represent mean values (± SEM) of τ determined in control conditions (open circles; $n = 9$) and in the presence of 10 μM (closed squares; $n = 5$), 200 μM (closed triangles; $n = 4$), and 1 mM neomycin (closed diamonds; $n = 3$). Lines are best fits to a monoexponential function.

inhibition was almost fully reversed (Fig.4 A, bottom, and Fig. 4 B). We performed dose–response experiments in the concentration range from 0.5 μM to 1 mM neomycin. In the presence of neomycin, macroscopic SV current amplitudes resulted from the combination of two opposing effects: (1) the voltage-dependent inhibition and (2) the shift of the activation threshold favoring channel opening, as described in the previous section. Taking this fact into account in the dose–response analysis, in order to evaluate the real blocking efficiency, we corrected the normalized currents obtained at different neomycin concentrations for the current increase due to SV activation at the respective concentration (for details see MATERIALS AND METHODS). Fitting the corrected data with the modified Hill equation $G_{neo}/G_{control} = (1 - I_r)/(1 + ([neo]/K_h)^n) + I_r$ (where [neo] is the neomycin concentration, K_h and n are the Hill constant and the Hill coefficient, respectively, and I_r is fraction of the residual current at saturating neomycin concentrations) revealed similar Hill coefficients for the investigated range of potentials (Fig. 5 A), indicating the same stoichiometry of the neomycin–SV interaction. We therefore subjected the data acquired at different potentials to a global Hill fit with the restriction of an identical Hill coefficient (Fig. 5 A), which turned out to be 0.66, indicative of a 1:1 stoichiometry. K_h values varied in a voltage-dependent manner in the high-affinity range from 3 to 10 μM (Fig. 5 B). The voltage dependence of K_h can be formally described by a monoexponential function (see line fit in Fig. 5 B): $K_h(V) = K_0 \exp(-z\partial FV/RT)$, where z is the valence of the blocking particle, and ∂ is the electrical distance the blocking particle has to traverse to reach its binding site; R, T, F, and V have their usual meanings. From this operation we obtained $K_0 = 78 \pm 20$ μM and $z\partial = 0.84 \pm 0.10$.

In view of previous findings that polyamines inhibit the SV channel from both sides of the vacuolar membrane (Dobrovinskaya et al., 1999b), we also performed preliminary experiments applying neomycin to the lumenal side of membrane patches (in the vacuolar side-out configuration). In the presence of 1 mM lumenal neomycin, macroscopic SV currents were reduced up to 50% (unpublished data). The effect was fully reversible.

Neomycin Reduces the Single Channel Conductance of the SV Channel

We investigated the basis of the observed macroscopic effects mediated by cytosolic neomycin on the single channel level under similar working conditions. To yield a higher single channel conductance we used a higher cytosolic K^+ concentration (200 mM), and we eliminated $Tris^+$ that was found to render clean single channel recordings difficult. This was probably due to the interaction of $Tris^+$ with the SV channel pore (Dobrovinskaya et al., 1999a). The $Tris^+$ concentration used for pH adjustment of our solutions for macroscopic current experiments was in the low millimolar range, which was shown to cause only a slight reduction of the single channel conductance (Dobrovinskaya et al., 1999a).

We used different strategies to gain information on the SV single channel conductance in a wide range of membrane potentials. Fig. 6 A shows SV single channel openings recorded at a slightly positive potential in control and in the presence of 50 μM neomycin. The trace in neomycin shows a fast flickering and a smaller amplitude of the channel's open state, thereby demonstrating exemplarily the two modes of neomycin action; as shown in a quantitative manner in the histograms of Fig. 6 B, neomycin on the one hand reduced the single channel conductance (shifted the peak of the open state to smaller current values, i.e., $i_{control} = 1.0$ pA; $i_{neo} = 0.5$ pA), and on the other hand increased the channel's open probability (increased the area related to the open state: $A_{neo}/A_{control} = 4.6$). The single channel current at negative membrane voltages was determined from SV deactivation events (Fig. 6 C). Again, a reduction of the unitary conductance and a flickering of the trace in the presence of neomycin became evident.

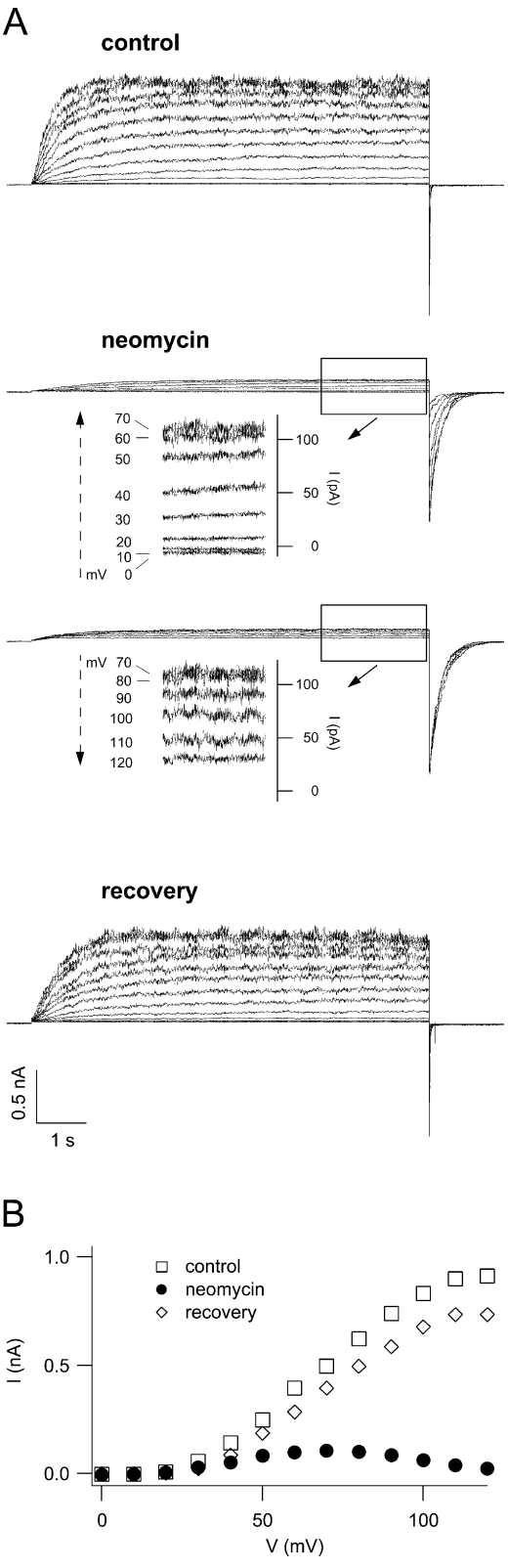

Figure 4. Neomycin inhibits SV currents in a voltage-dependent manner. (A) Macroscopic SV currents, elicited by a series of voltage steps ranging from 0 to +120 mV, were recorded from a cytosolic side-out patch in control (top) and in are split into the voltage range from 0 to +70 mV (second panel) and from +70 to +120 mV (third panel). Insets show a magnification of the original traces at the end of the activating pulse (rectangle). The bottom panel shows the recovery. Holding and tail potentials were at −50 and −80 mV, respectively. (B) SV current–voltage relationships in control (open squares), in the presence of 1 mM neomycin (filled circles), and after recovery (open diamonds), obtained from the traces shown in A by plotting stationary current values as a function of the applied voltage.

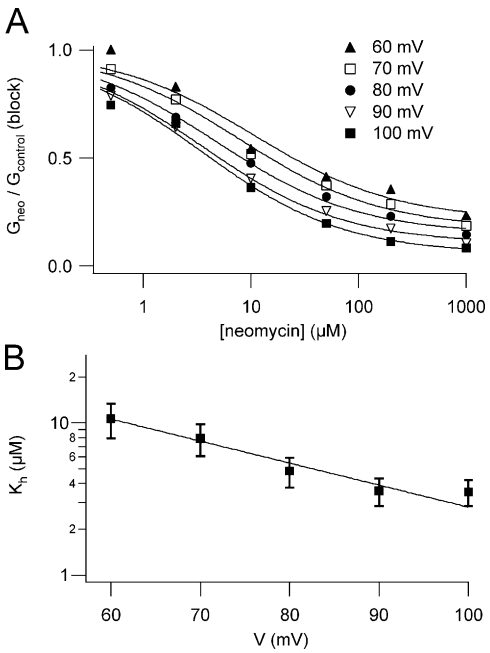

Figure 5. Quantitative analysis of SV channel block by neomycin. (A) Dose–response of block in the voltage range from +60 to +100 mV; normalized stationary currents for six neomycin concentrations derived from three to five experiments were averaged, corrected for current increase due to neomycin-induced channel activation, as described in MATERIALS AND METHODS, and resulting $G_{neo}/G_{control}$(block) values were plotted as a function of neomycin concentration. For all potentials under investigation, a global curve fit was performed, which allowed the fit of all data sets with the same Hill coefficient and a series of Hill functions. Values of I_r, the fraction of the residual current at saturating neomycin concentrations, were as follows: 0.21 ± 0.04 at +60 mV, 0.17 ± 0.03 at +70 mV, 0.15 ± 0.03 at +80 mV, 0.11 ± 0.03 at +90 mV, 0.06 ± 0.03 at +100 mV. (B) K_h values derived from the Hill global fit shown in A are plotted against the applied membrane potential. The line represents the best fit with a monoexponential function.

Resulting current values derived from recordings like the ones shown in Fig. 6 (A and C) are summarized in Fig. 7 A. At negative potentials, the reduction of the single channel current caused by the presence of neomycin seemed to be fairly voltage independent, while at slightly positive potentials, the reduction increased with the applied voltage. Finally, we applied a fast voltage ramp protocol to single open channels (Fig. 7 B), in order to get access to the unitary conductance at far positive potentials where single channel events cannot be resolved because of the high number of open channels. The presence of neomycin in the bath caused a strong voltage-dependent reduction of the single channel

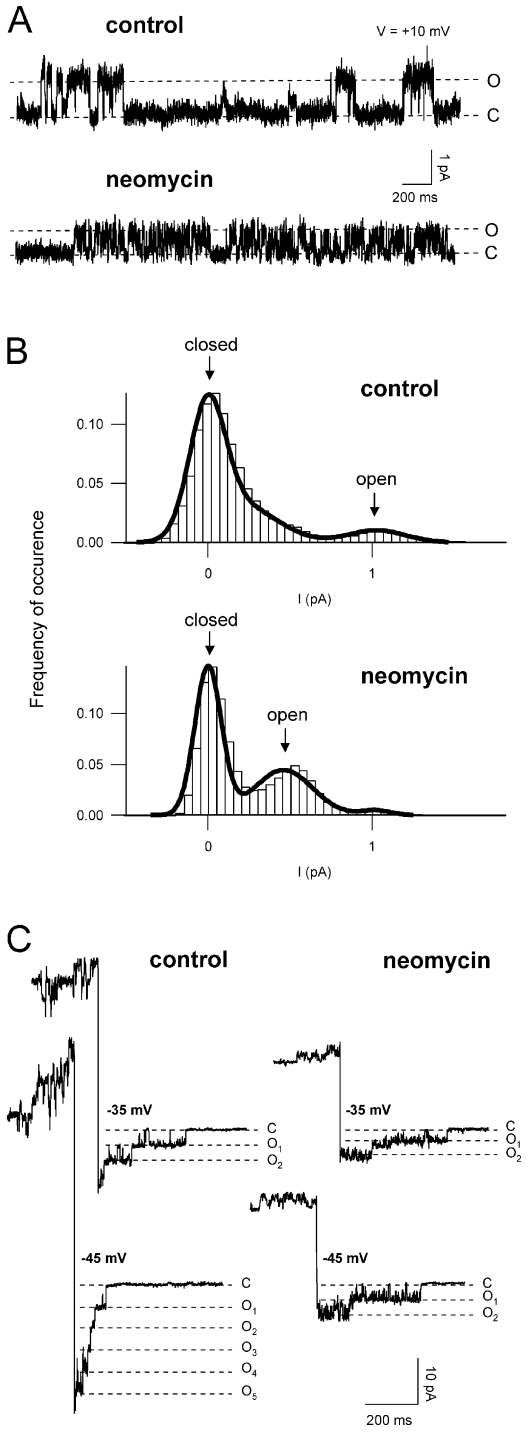

Figure 6. Neomycin reduces the single channel conductance of the SV channel. (A) Representative single channel recordings in control (top trace) and in the presence of 50 μM neomycin (bottom trace). The closed (C) and open (O) state levels are indicated by dotted lines. Currents were recorded from a cytosolic side-out vacuolar patch in bath and pipette solutions containing 200 mM K^+. Applied potential +10 mV, sampling time 200 μs, filter 5 kHz. (B) Single channel amplitude distributions derived from strip records (as in A) in control (top panel) and in the presence of 50 μM neomycin (bottom panel). Note the decreased distance between the closed and open state peaks as wellas the area increase corresponding to the open state in the presence of neomycin. Record length 50 s, bin size 0.05 pA. (C) Recordings showing single SV deactivation events in control (left traces) and in the presence of 50 μM neomycin (right traces) at selected potentials. The closed (C) and different open (O_1, O_2, O_3, etc.) state levels are indicated by dotted lines. Holding potentials were at +40 mV in control and +30 mV in neomycin.

current, leading to a complete channel block at elevated positive potentials (Fig. 7 B). As shown in the same figure, superimposed data from Fig. 7 A perfectly matched the course of the voltage ramp traces of both control and neomycin.

In order to compare these single channel data to the blocking efficiency of neomycin revealed on the macroscopic current level, we applied the blocking parameters obtained by the fit in Fig. 5 B to the control data in Fig. 7. The current in the presence of neomycin is then given by: $i_{neo} = gV(1/(1 + ([neo]/K_h(V))^n))$, where g is the single channel conductance in control condition (g = 104 pS; from linear fit in Fig. 7 A), and [neo] is the neomycin concentration used (50 μM). $K_h(V)$ and n are derived from macroscopic current data shown in Fig. 5.

Notably, the graph of this function (dashed lines in Fig. 7, A and B) is in very good agreement with the experimental data in the whole voltage range investigated. Most interestingly, it also predicts the slight reduction of single channel currents at negative membrane potentials.

Kanamycin Blocks SV Channels Less Effectively than Neomycin

The experiments presented thus far demonstrated two opposing modes of neomycin action on the SV channel: (1) an increase of the channel's open probability favoring channel activation at more negative membrane potentials and (2) a voltage-dependent reduction of the single channel conductance leading to an inhibition of macroscopic currents at positive membrane potentials. In recordings of macroscopic SV currents, these two effects are superimposed. It is well established that SV channel block by polyamines is dependent on their net charge (Dobrovinskaya et al., 1999b). Thus, it was tempting to speculate that it may be possible to modulate the relative contribution of the two modes of neomycin action by using a compound structurally related to neomycin, but with a smaller net charge at pH 7.5. In contrast to neomycin B, kanamycin A is an antibiotic of the 4,6-disubstituted aminoglycoside subclass (Fig. 1), with only four amine groups and a net charge of +1.7 at pH 7.4 (Yeiser et al., 2004). Applied at a concentration of 1 mM to the bath solution, kanamycin had a stimulatory effect on macroscopic SV currents at membrane potentials <+80 mV, which progressively decreased and eventually turned into an inhibitory effect with increasing voltage (Fig. 8, A and B). In Fig. 8 B, data points obtained in the presence of 1 mM neomycin B, which entered the dose–response

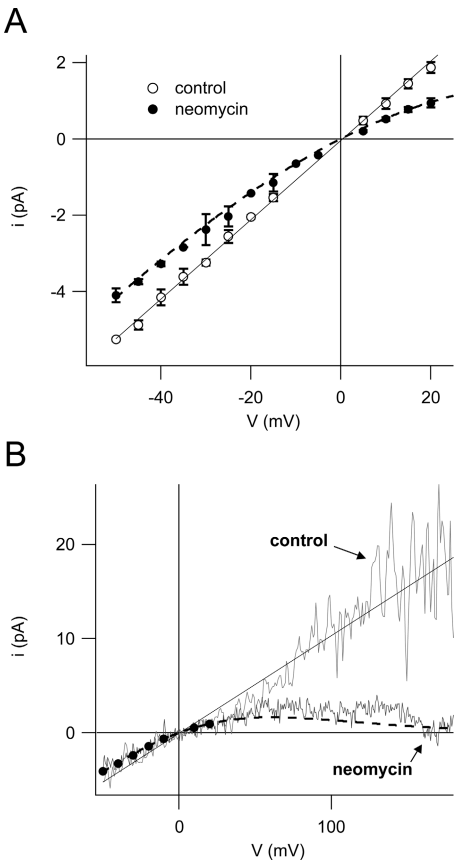

Figure 7. SV channels are completely blocked by neomycin at high positive membrane potentials. (A) Single channel current–voltage relationship in control conditions (open circles) and in the presence of 50 μM neomycin (filled circles) derived from continuous traces for positive potentials (e.g., Fig. 6 A) and from deactivation tails for negative potentials (e.g., Fig. 6 C) of two to four experiments (error bars represent SD). Data points of control were fitted with a linear function (black line) yielding a unitary conductance of 104 ± 1 pS. (B) Individual single channel current–voltage relationships in control (light gray trace) and 50 μM neomycin (dark gray trace) obtained from a cytosolic side-out excised patch. Traces were superimposed with data points for neomycin (filled circles) and the linear fit for control (both from A). Dashed lines in A and B are the graphical representation of the function predicting single channel currents in the presence of 50 μM neomycin on the basis of fit parameters derived from dose–response analyses of macroscopic currents (Fig. 5). See text for details.

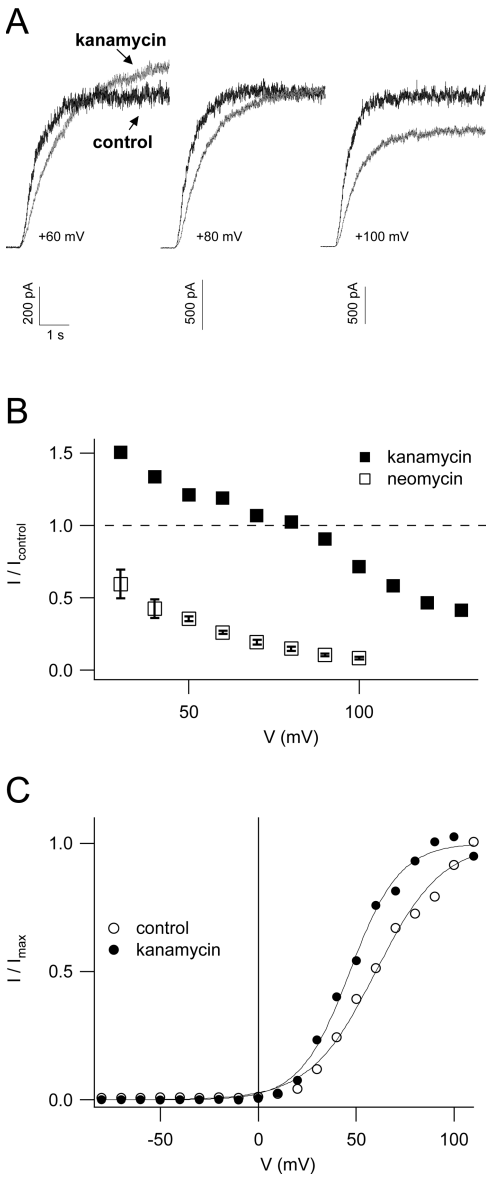

Figure 8. Kanamycin blocks SV channels less effectively than neomycin. (A) Representative macroscopic SV currents in control conditions (black traces) and in the presence of 1 mM kanamycin (gray traces), elicited by voltage steps to +60 mV (left), +80 mV (middle), and +100 mV (right) from a holding potential of 0 mV. (B) Currents (from the same experiment shown in A) recorded in the presence of 1 mM kanamycin (filled squares) were normalized to the respective control current value and plotted against the applied membrane potential. Mean values (± SEM) obtained in the presence of 1 mM neomycin (open squares), which entered into the dose–response analysis for neomycin (see Fig. 5), are reported for comparison. (C) Boltzmann analysis of instantaneous tail currents recorded in control (open circles) and in the presence of 1 mM kanamycin (closed circles). Current values were plotted as a function of the activating potential, fitted with a Boltzmann function, and normalized to the saturating current level. Fit parameters were for control: $V_{1/2}$ = +60 mV, z = 1.49, I_{max} = +3.3 nA; for kanamycin: $V_{1/2}$ = +47 mV, z = 1.99, I_{max} = +4.3 nA.

analysis of neomycin block (see Fig. 5), demonstrate that kanamycin A was indeed far less effective in blocking SV channels than neomycin B. Boltzmann analysis of instantaneous tail currents, shown in Fig. 8 C, revealed a shift of the SV activation threshold of 13 mV towards negative potentials in the presence of kanamycin, which is presumably responsible for the stimulation of macroscopic currents at small membrane potentials (Fig. 8, A and B).

DISCUSSION

This work on the interaction between the aminoglycoside neomycin B and the slow vacuolar channel from

Arabidopsis mesophyll cells provided two major findings: neomycin (1) blocked the channel in a voltage- dependent manner and (2) shifted the threshold of channel activation to more negative values.

Voltage-dependent Block of SV Currents

Inhibition of SV macroscopic currents depended on the concentration of neomycin and the applied membrane potential. Dose–response analyses of these data suggested a voltage-dependent Hill constant K_h and a 1:1 stoichiometry of the interaction between neomycin and the channel protein, which is not surprising in consideration of the relative large size of the neomycin molecule (MW = 615) and was also reported in the interaction of neomycin with animal sodium channels (Yeiser et al., 2004) and L-type calcium channels (Haws et al., 1996). At the single channel level, neomycin at a concentration of 50 μM caused a voltage-independent reduction of the channel conductance at negative membrane potentials. The reduced cytosol-directed flux seems to be incompatible with a decrease of the local concentration of permeating ions at the cytoplasmic pore entrance owing to the repulsive action of neomycin. Possibly, neomycin partially obstructs the permeation pathway also at negative membrane potentials. The reduction of single channel conductance increased dramatically at progressively more positive potentials (Fig. 7 B); this provides evidence for a pore block due to binding of positively charged amino groups of the neomycin molecule at a site located within the electrical field of the ion-conducting pathway, as described for neomycin block of other cation channels (Nomura et al., 1990; Haws et al., 1996; Winegar et al., 1996; Mead and Williams, 2002; Yeiser et al., 2004). Indeed, the much slower channel deactivation at negative membrane potentials in the presence of neomycin (Fig. 3 B) may indicate a voltage-driven unblocking of the pore, explainable with a foot-in-the-door mechanism (Yeh and Armstrong, 1978; Yellen, 1998). Furthermore, this mechanism of neomycin block is in perfect agreement with a previous report showing that polyamines are able to enter into the SV pore and even to permeate at large positive potentials (Dobrovinskaya et al., 1999a). Most intriguingly, the reduction of single channel conductance in the whole range of investigated potentials, both negative and positive, could be very well predicted by the blocking parameters $K_h(V)$ and n, obtained from macroscopic current experiments (Fig. 5). This prediction allowed us to deduce the following: (a) the reduced conductance at negative potentials is essentially due to the fact that the applied neomycin concentration (50 μM) is comparable to the K_h value at V = 0, i.e., 78 μM, and (b) the value of $z\partial$ (0.84) determined the strong voltage-dependent reduction conductance at positive potentials.

Also the dynamic fingerprinting of the SV channel changed significantly on the addition of neomycin, displaying a rapid intrachannel flickering at positive potentials as well as at negative tail potentials (following a positive stimulation pulse). This flickering further supports the hypothesis of a tight interaction of neomycin with the pore, which could be responsible for the strong decrease of the unitary current at positive potentials. The presence of too many channels in excised patches restricted our analysis of single channel events to the range of slightly positive membrane potentials. Contrary to what has been observed in neomycin interaction with other channels (Winegar et al., 1996; Mead and Williams, 2002), a preliminary single channel analysis did not provide any evidence for a systematically occurring subconductance state induced by neomycin nor for direct consequences of the flickering on the reduced channel amplitude; instead, both single channel recognition and noise analysis (unpublished data) confirmed that the flickering represents a fast, temporary block of the pore occurring during longer SV channel openings and giving rise to prolonged channel bursts. Similarly to what has been suggested for the block induced by verapamil on the large-conductance Ca^{2+}-activated K^+ channel (Harper et al., 2001), these prolonged channel bursts observable at positive and negative tail potentials in the presence of neomycin strongly support the possibility that when the blocker is bound to the (open) pore, the channel becomes kinetically frozen in a flickery open-blocked state and cannot make transitions towards other (closed) states. Unfortunately, the presence of too many channels in excised patches did not allow the investigation of the effects of flickering at very positive membrane potentials.

So far, we cannot exclude contributions of surface charge screening to the decrease of the conductance at positive potentials and the possibility that the channel flickering may be ascribed to an allosteric mechanism modifying the channel's structure and kinetic properties. A more detailed single channel analysis needs to be performed to clarify these points.

The blocking strength of kanamycin A was clearly smaller than the one of neomycin; this is in agreement with the correlation between the net charge of naturally occurring polyamines and their capability to block SV channels (Dobrovinskaya et al., 1999b). An analogous relationship between the number of amine groups of aminoglycosides and their blocking potency was postulated for animal Ca^{2+}-activated potassium channels (Nomura et al., 1990) and L-type calcium channels (Haws et al., 1996). However, no such correlation was found for sodium channels (Yeiser et al., 2004), favoring alternative hypotheses on the binding of aminoglycosides based on the size of the molecule or on the location of the amine groups.

Neomycin determined a voltage-dependent block of the cardiac ryanodine receptor (RyR) acting both at the cytosolic and lumenal mouth of the pore (Mead and Williams, 2002; Mead and Williams, 2004). In the context of this study, it is interesting to note that neomycin has been proposed to be a fitting plug in the RyR pore and also that, under appropriate conditions, it is capable to pass through the RyR pore (Mead and Williams, 2002). It has been furthermore demonstrated that neomycin, and other aminoglycoside antibiotics, reduce the unitary current of a mechanosensitive channel from mouse muscle fibre, causing a fast flickering of the channel, a subconductance level, and an incomplete obstruction of the pore (Winegar et al., 1996). These similarities strongly support the assumption that equivalent tight interactions also occur within the SV pore.

SV Channel Activation

SV channels show pronounced outward rectifying properties, activating at potentials more positive than the presumed physiological tonoplast potential. Major cellular factors that were reported to shift the activation threshold of the channel are the divalent cations Ca^{2+} and Mg^{2+}. As cytosolic calcium is an indispensable activator of the SV channel, a concentration increase in the cytosol greatly favors channel opening (Hedrich and Neher, 1987), while it has the opposite effect, i.e., it shifts the activation threshold to more positive potentials, when present on the vacuolar side of the membrane (Pottosin et al., 2004). The lower affinity of Mg^{2+} to the SV channel renders this cation less efficient than Ca^{2+} in modulating the channel (Pei et al., 1999; Carpaneto et al., 2001; Pottosin et al., 2004). Due to its high effectiveness, vacuolar calcium was proposed to have a prominent role in controlling SV activity (Pottosin et al., 2004). Interestingly, channel activation at negative potentials was only observed when working without or with low (micromolar) concentrations of vacuolar calcium (Pottosin et al., 1997; Pei et al., 1999; Ivashikina and Hedrich, 2005). In contrast, the results shown here were obtained in the presence of 2 mM vacuolar calcium. Clearly, neomycin is able to activate the SV channel at negative membrane potentials, even under these unfavorable conditions for channel opening.

What could be the mechanism by which neomycin produces a shift of the activation characteristics? Neomycin may compete with Ca^{2+} for its cytosolic binding site on the channel, displace it, and shift the activation curve towards more negative voltages (Pottosin et al., 1997; Carpaneto et al., 2001). This would indicate that the affinity of neomycin to this site is extraordinarily high, given that shift saturation is reached at 10 μM neomycin in the presence of 100-fold excess of calcium. However, while an increase of cytosolic calcium typically accelerates channel activation and deactivation (Carpaneto et al., 2001), neomycin had the opposite effect on kinetic parameters (Fig. 3), which argues against a common binding site.

Another possibility could be that the presence of the positively charged neomycin molecule leads to a shift of the activation voltage by simply screening negative surface charges on the vacuolar membrane. In this case one should expect that the addition of neomycin determines faster activation and slower deactivation of the channel. On the contrary, experimental data (Fig. 3) showed that neomycin slows down both kinetic parameters. Alternatively, the slower activation in the presence of neomycin could be explained by a binding to the channel protein, which affects the movement of the voltage sensor, owing either to steric hindrance or to electrostatic interaction.

Recordings on the single channel level showing a reduced unitary conductance and an increase in the open probability in the presence of neomycin provided a consistent explanation for the observed macroscopic current changes. Interestingly, these two features were at first sight reminiscent of the effects of neomycin on mammalian NMDA-gated ionotropic glutamate receptors (Lu et al., 1998), the only channel class previously known to be activated by aminoglycosides. The activating property of neomycin has been explained by the finding that many structurally diverse polyamines can mimic the physiological actions of endogenous polyamines, like spermine, on NMDA receptors, which involve an increase of the frequency of channel opening and an increase of the channel's affinity for its activator glycine (Pullan et al., 1992; Rock and Macdonald, 1995). In the case of the SV channel, however, this explanation cannot hold true, as endogenously occurring polyamines were found to inhibit SV currents, but not to have activating effects (Dobrovinskaya et al., 1999b). In this context it is remarkable that a recent study reported that *Arabidopsis* glutamate receptors, the plant homologues of NMDA receptors, may indeed be targeted by polyamines and aminoglycosides like kanamycin, indicating a high degree of conservation between animals and plants (Dubos et al., 2005). In view of the facts that the SV channel protein, recently identified as TPC1 (Peiter et al., 2005), belongs to the family of voltage-gated two-pore channels and not to the ligand-gated glutamate receptor family, and moreover does not contain the amino acid signature implicated in polyamine and aminoglycoside binding to NMDA receptors (Masuko et al., 1999; Huggins and Grant, 2005), one may expect a different mechanism of neomycin action on the SV channel. Our results demonstrated that the activating effect of neomycin is composed of two phenomena. Boltzmann analyses revealed, firstly, a shift of the voltage dependence to more negative potentials saturating at a neomycin concentration of 10–50 μM, which could be explained by an increase of the open probability of the channel, and secondly, the manifestation of an

additional gating process at higher concentrations giving rise to significant channel opening at negative membrane potentials.

Physiological and Biophysical Implications

Our results provide the first evidence of SV channel activation at physiological tonoplast potentials elicited by an organic effector molecule. They further support the existence of a cellular helper factor that is able to shift the activation potential of the SV channel in vivo, as already proposed by other authors (Pei et al., 1999; Carpaneto et al., 2001). Based on their structural similarity, endogenous polyamines like spermine, spermidine, and putrescine are the most obvious candidates. But, as already outlined above, these compounds had no effect on the open probability of the SV channel (Dobrovinskaya et al., 1999b). If not by themselves, they may possibly act together with yet another cellular factor or protein, as has been suggested for the regulation of plasma membrane inward K^+ channels in guard cells (Liu et al., 2000).

The finding that neomycin is capable of activating the Ca^{2+}-permeable SV channel receives further significance from the channel's implication in the release of vacuolar calcium during cellular signaling in plants (Ward and Schroeder, 1994), as it could interfere with experiments employing aminoglycosides to study other (calcium) signaling pathways. Most importantly, neomycin is a widely used antagonist of IP_3-dependent intracellular calcium release, based on its inhibition of phosphoinositide-specific PLC. This enzyme catalyzes the formation of the second messengers diacylglycerol and inositol IP_3. The latter was shown to have high-affinity binding sites at the tonoplast (Brosnan and Sanders, 1993) and to activate a calcium channel (Alexandre et al., 1990) promoting Ca^{2+} release from isolated vacuoles. IP_3-dependent increases in cytosolic Ca^{2+} have been implicated, e.g., in ABA-induced stomatal closure (Hunt et al., 2003) and cellular responses to blue light (Harada et al., 2003). In light of our results, it may be advisable not to rely solely on neomycin in inhibitor studies on IP_3-dependent calcium release, but to employ other structurally unrelated inhibitors.

Furthermore, kanamycin was recently found to rescue the phenotype of dark-grown *Arabidopsis de-etiolated3* (*det3*) mutant plants (Dubos et al., 2005). The results of several experimental approaches suggested a model in which the activation of glutamate receptor channels by the aminoglycoside suppresses the excessive expression of the transcription factor *AtMYB61* in the *det3* mutant (Dubos et al., 2005). Although the authors did not further discuss the mechanistic link between glutamate receptor activation and *AtMYB61* down-regulation, this may consist in an increase in cytosolic calcium. Both glutamate receptors and SV channels are nonselective cation channels (Davenport, 2002; Demidchik et al., 2002), potentially capable of triggering this signal. Thus, it cannot be excluded that a minor part of the signal leading to the observed phenotypical changes is attributable to SV activation by kanamycin.

Finally, the results of this study emphasize the usefulness of aminoglycosides, or similar electrically charged molecules, as probes to investigate the functional and structural properties of the SV channel pore region. In this sense, neomycin might prove to be as valuable as it is the alkaloid ryanodine for the study of animal ryanodine receptor channels. The intriguing effects of this molecule class may also serve to confirm the identity of the SV channel protein recently reported as TPC1 (Peiter et al., 2005).

This research was supported by the EU-RTN project "Novel Ion Channels in Plants" (HPRN-CT-2002-00245).

Olaf S. Andersen served as editor.

Submitted: 13 September 2005
Accepted: 8 February 2006

REFERENCES

Alexandre, J., J.P. Lassalles, and R.T. Kado. 1990. Opening of Ca^{2+} channels in isolated red beet root vacuole membrane by inositol 1,4,5-trisphosphate. *Nature.* 343:567–570.

Allen, G.J., and D. Sanders. 1996. Control of ionic currents in guard cell vacuoles by cytosolic and luminal calcium. *Plant J.* 10:1055–1069.

Allen, G.J., and D. Sanders. 1997. Vacuolar ion channels. *Adv. Bot. Res.* 25:217–252.

Amodeo, G., A. Escobar, and E. Zeiger. 1994. A cationic channel in the guard cell tonoplast of *Allium cepa*. *Plant Physiol.* 105:999–1006.

Bertl, A., and C.L. Slayman. 1990. Cation-selective channels in the vacuolar membrane of *Saccharomyces*: dependence on calcium, redox state, and voltage. *Proc. Natl. Acad. Sci. USA.* 87:7824–7828.

Bertl, A., E. Blumwald, R. Coronado, R. Eisenberg, G. Findlay, D. Gradmann, B. Hille, K. Kohler, H.A. Kolb, E. MacRobbie, et al. 1992. Electrical measurements on endomembranes. *Science.* 258: 873–874.

Brosnan, J.M., and D. Sanders. 1993. Identification and characterization of high-affinity binding sites for inositol trisphosphate in red beet. *Plant Cell.* 5:931–940.

Carpaneto, A., A.M. Cantu, and F. Gambale. 1999. Redox agents regulate ion channel activity in vacuoles from higher plant cells. *FEBS Lett.* 442:129–132.

Carpaneto, A., A.M. Cantu, and F. Gambale. 2001. Effects of cytoplasmic Mg^{2+} on slowly activating channels in isolated vacuoles of *Beta vulgaris*. *Planta.* 213:457–468.

Davenport, R. 2002. Glutamate receptors in plants. *Ann. Bot. (Lond.).* 90:549–557.

Demidchik, V., R.J. Davenport, and M. Tester. 2002. Nonselective cation channels in plants. *Annu. Rev. Plant Biol.* 53:67–107.

Dobrovinskaya, O.R., J. Muniz, and I.I. Pottosin. 1999a. Asymmetric block of the plant vacuolar Ca^{2+}-permeable channel by organic cations. *Eur. Biophys. J.* 28:552–563.

Dobrovinskaya, O.R., J. Muniz, and I.I. Pottosin. 1999b. Inhibition of vacuolar ion channels by polyamines. *J. Membr. Biol.* 167:127–140.

Downes, C.P., and R.H. Michell. 1981. The polyphosphoinositide phosphodiesterase of erythrocyte membranes. *Biochem. J.* 198:133–140.

Dubos, C., J. Willment, D. Huggins, G.H. Grant, and M.M. Campbell. 2005. Kanamycin reveals the role played by glutamate receptors in shaping plant resource allocation. *Plant J.* 43:348–355.

Gabev, E., J. Kasianowicz, T. Abbott, and S. McLaughlin. 1989. Binding of neomycin to phosphatidylinositol 4,5-bisphosphate (PIP2). *Biochim. Biophys. Acta.* 979:105–112.

Gambale, F., M. Bregante, F. Stragapede, and A.M. Cantu'. 1996. Ionic channels of the sugar beet tonoplast are regulated by a multi-ion single-file permeation mechanism. *J. Membr. Biol.* 154:69–79.

Harada, A., T. Sakai, and K. Okada. 2003. Phot1 and phot2 mediate blue light-induced transient increases in cytosolic Ca^{2+} differently in *Arabidopsis* leaves. *Proc. Natl. Acad. Sci. USA.* 100:8583–8588.

Harper, A.A., L. Catacuzzeno, C. Trequattrini, A. Petris, and F. Franciolini. 2001. Verapamil block of large-conductance Ca-activated K channels in rat aortic myocytes. *J. Membr. Biol.* 179: 103–111.

Haws, C.M., B.D. Winegar, and J.B. Lansman. 1996. Block of single L-type Ca^{2+} channels in skeletal muscle fibers by aminoglycoside antibiotics. *J. Gen. Physiol.* 107:421–432.

Hedrich, R., and E. Neher. 1987. Cytoplasmic calcium regulates voltage-dependent ion channels in plant vacuoles. *Nature.* 329:833–835.

Huggins, D.J., and G.H. Grant. 2005. The function of the amino terminal domain in NMDA receptor modulation. *J. Mol. Graph. Model.* 23:381–388.

Hunt, L., L.N. Mills, C. Pical, C.P. Leckie, F.L. Aitken, J. Kopka, B. Mueller-Roeber, M.R. McAinsh, A.M. Hetherington, and J.E. Gray. 2003. Phospholipase C is required for the control of stomatal aperture by ABA. *Plant J.* 34:47–55.

Ivashikina, N., and R. Hedrich. 2005. K+ currents through SV-type vacuolar channels are sensitive to elevated luminal sodium levels. *Plant J.* 41:606–614.

Liu, K., H. Fu, Q. Bei, and S. Luan. 2000. Inward potassium channel in guard cells as a target for polyamine regulation of stomatal movements. *Plant Physiol.* 124:1315–1326.

Lu, W.Y., Z.G. Xiong, B.A. Orser, and J.F. MacDonald. 1998. Multiple sites of action of neomycin, Mg^{2+} and spermine on the NMDA receptors of rat hippocampal CA1 pyramidal neurones. *J. Physiol.* 512(Pt 1):29–46.

Masuko, T., K. Kashiwagi, T. Kuno, N.D. Nguyen, A.J. Pahk, J. Fukuchi, K. Igarashi, and K. Williams. 1999. A regulatory domain (R1-R2) in the amino terminus of the N-methyl-D-aspartate receptor: effects of spermine, protons, and ifenprodil, and structural similarity to bacterial leucine/isoleucine/valine binding protein. *Mol. Pharmacol.* 55:957–969.

Mead, F., and A.J. Williams. 2002. Block of the ryanodine receptor channel by neomycin is relieved at high holding potentials. *Biophys. J.* 82:1953–1963.

Mead, F.C., and A.J. Williams. 2004. Electrostatic mechanisms underlie neomycin block of the cardiac ryanodine receptor channel (RyR2). *Biophys. J.* 87:3814–3825.

Mingeot-Leclercq, M.P., Y. Glupczynski, and P.M. Tulkens. 1999. Aminoglycosides: activity and resistance. *Antimicrob. Agents Chemother.* 43:727–737.

Moazed, D., and H.F. Noller. 1987. Interaction of antibiotics with functional sites in 16S ribosomal RNA. *Nature.* 327:389–394.

Nomura, K., K. Naruse, K. Watanabe, and M. Sokabe. 1990. Aminoglycoside blockade of Ca^{2+}-activated K^+ channel from rat brain synaptosomal membranes incorporated into planar bilayers. *J. Membr. Biol.* 115:241–251.

Pantoja, O., A. Gelli, and E. Blumwald. 1992. Voltage-dependent calcium channels in plant vacuoles. *Science.* 255:1567–1570.

Pei, Z.M., J.M. Ward, and J.I. Schroeder. 1999. Magnesium sensitizes slow vacuolar channels to physiological cytosolic calcium and inhibits fast vacuolar channels in fava bean guard cell vacuoles. *Plant Physiol.* 121:977–986.

Peiter, E., F.J. Maathuis, L.N. Mills, H. Knight, J. Pelloux, A.M. Hetherington, and D. Sanders. 2005. The vacuolar Ca^{2+}-activated channel TPC1 regulates germination and stomatal movement. *Nature.* 434:404–408.

Pichler, M., Z. Wang, C. Grabner-Weiss, D. Reimer, S. Hering, M. Grabner, H. Glossmann, and J. Striessnig. 1996. Block of P/Q-type calcium channels by therapeutic concentrations of aminoglycoside antibiotics. *Biochemistry.* 35:14659–14664.

Pottosin, I.I., L.I. Tikhonova, R. Hedrich, and G. Schönknecht. 1997. Slowly activating vacuolar channels cannot mediate Ca^{2+}-induced Ca^{2+} release. *Plant J.* 12:1387–1398.

Pottosin, I.I., O.R. Dobrovinskaya, and J. Muniz. 2001. Conduction of monovalent and divalent cations in the slow vacuolar channel. *J. Membr. Biol.* 181:55–65.

Pottosin, I.I., M. Martinez-Estevez, O.R. Dobrovinskaya, J. Muniz, and G. Schonknecht. 2004. Mechanism of luminal Ca^{2+} and Mg^{2+} action on the vacuolar slowly activating channels. *Planta.* 219:1057–1070.

Pullan, L.M., R.J. Stumpo, R.J. Powel, K.A. Paschetto, and M. Britt. 1992. Neomycin is an agonist at a polyamine site on the N-methyl-D-aspartate receptor. *J. Neurochem.* 59:2087–2093.

Raisinghani, M., and L.S. Premkumar. 2005. Block of native and cloned vanilloid receptor 1 (TRPV1) by aminoglycoside antibiotics. *Pain.* 113:123–133.

Reifarth, F.W., T. Weiser, and F.W. Bentrup. 1994. Voltage- and Ca^{2+}-dependence of the K^+ channel in the vacuolar membrane of *Chenopodium rubrum* L. suspension cells. *Biochim. Biophys. Acta.* 1192:79–87.

Rock, D.M., and R.L. Macdonald. 1995. Polyamine regulation of N-methyl-D-aspartate receptor channels. *Annu. Rev. Pharmacol. Toxicol.* 35:463–482.

Rothlin, C.V., E. Katz, M. Verbitsky, D.E. Vetter, S.F. Heinemann, and A.B. Elgoyhen. 2000. Block of the α9 nicotinic receptor by ototoxic aminoglycosides. *Neuropharmacology.* 39:2525–2532.

Scholz-Starke, J., A. De Angeli, C. Ferraretto, S. Paluzzi, F. Gambale, and A. Carpaneto. 2004. Redox-dependent modulation of the carrot SV channel by cytosolic pH. *FEBS Lett.* 576:449–454.

Scholz-Starke, J., A. Naso, and A. Carpaneto. 2005. A perspective on the slow vacuolar channel in vacuoles from higher plant cells. *J. Chem. Inf. Model.* 45:1502–1506.

Schulz-Lessdorf, B., and R. Hedrich. 1995. Protons and calcium modulate SV-type channels in the vacuolar-lysosomal compartment-channel interaction with calmodulin inhibitors. *Planta.* 197: 655–671.

Shi, L.J., L.A. Liu, X.H. Cheng, and C.A. Wang. 2002. Decrease in acetylcholine-induced current by neomycin in PC12 cells. *Arch. Biochem. Biophys.* 403:35–40.

Ward, J.M., and J.I. Schroeder. 1994. Calcium-activated K+ channels and calcium-induced calcium release by slow vacuolar ion channels in guard cell vacuoles implicated in the control of stomatal closure. *Plant Cell.* 6:669–683.

Winegar, B.D., C.M. Haws, and J.B. Lansman. 1996. Subconductance block of single mechanosensitive ion channels in skeletal muscle fibers by aminoglycoside antibiotics. *J. Gen. Physiol.* 107:433–443.

Woodcock, J., D. Moazed, M. Cannon, J. Davies, and H.F. Noller. 1991. Interaction of antibiotics with A- and P-site-specific bases in 16S ribosomal RNA. *EMBO J.* 10:3099–3103.

Yeh, J.Z., and C.M. Armstrong. 1978. Immobilization of gating charge by a substance that simulates inactivation. *Nature.* 273:387–389.

Yeiser, A.J., J.R. Cox, and S.N. Wright. 2004. Voltage-dependent inhibition of rat skeletal muscle sodium channels by aminoglycoside antibiotics. *Pflugers Arch.* 448:204–213.

Yellen, G. 1998. The moving parts of voltage-gated ion channels. *Q. Rev. Biophys.* 31:239–295.